Selective communication and information processing by excitable systems

V. B. Kazantsev
Radiophysical Department, Nizhny Novgorod State University, 23 Gagarin Avenue, 603950 Nizhny Novgorod, Russia
(Received 6 March 2001; published 19 October 2001)

The phenomena of selective response of an excitable system to external pulse stimulation relating to interneuron communication and information processing problems are discussed. Subthreshold dynamics of the FitzHugh-Nagumo-like excitable system modeling of a neuron with the synaptic input is investigated. It is shown that the system response on various incoming information messages can be described by one- and two-dimensional linear and nonlinear point maps. Nonlinear integrating and resonant properties of the system are analyzed.

DOI: 10.1103/PhysRevE.64.056210 PACS number(s): 05.45.−a, 87.10.+e, 07.05.−t

I. INTRODUCTION

The problems of interneuron communication and information processing in central nervous system (CNS) have been intensively studied in recent years. The investigation of information pathways in CNS, the functions of synaptic transmission, information encoding, and communication concerns both fundamental scientific understanding of global CNS functions and related applications [1–9]. Then, the design of artificial systems based on the principles of neurodynamics intensively develops in connection with possible engineering applications. Take, for instance, cellular neural networks, reaction-diffusion lattices, optical neurocomputers, etc. [10–18]

At single cell level the problem of neuron communication concerns the dynamics of a neuron stimulated by pulse sequences with variable interspike interval that represent, in fact, encoded information messages [2–8]. Typically, the single neuron may have one or many different synaptic connections with other neurons and should produce adequate response on various incoming signals. From the behavioral or functional point of view there are two major types of the response [2–5]. The first type (*integrate-and-fire neurons*) summarizes or integrates the incoming signals and when reaching the excitation threshold generates the response pulse. The number of input pulses to be integrated is defined by the interspike interval characterizing the message and by the intrinsic characteristics of the cell. Neurons of the second type exhibit a resonant response. They fire when the spike frequency is in a resonant relation with the intrinsic frequencies of the cell [2–5,19,20]. Such neurons can communicate only at selective frequencies [3–5]. Recent experiments have confirmed that the resonant neurons play the key role in functional neuronal circuits responsible for different global functions of the CNS. For example, the thalamocortical circuit responsible for the associative memory CNS function uses $\sim$40 Hz frequency, the olivocerebellar circuit at $\sim$10 Hz plays a crucial role in the motor performance and movement coordination [2,3].

In modeling, various dynamical systems accounting for functional properties of real neurons can be used [5]. In particular, for integrating response one can use FitzHugh-Nagumo-like excitable systems with relaxation dynamics. Resonant response may occur in the systems oscillating below the threshold at a limit cycle (true oscillations) or near a fixed point of focus type (damped oscillations).

In this paper I consider an excitable dynamical system of FitzHugh-Nagumo type capable of *integrating, resonant, and integrating at resonance* responses on various information messages. It is shown that the problem of the response can be reduced to the analysis of 1D (one-dimensional) and 2D linear and nonlinear point maps. Section II describes the model, its phase space and basic properties. In Sec. III the 1D nonlinear point map describing nonlinear integrating response is analytically obtained and analyzed. Section IV is devoted to possible responses on stimulation when the system exhibits damped oscillation. In the linear approximation the 2D point map describing basic resonant properties is derived. Nonlinear resonance response is analyzed with the 2D nonlinear map. Section V illustrates the possibility of response on ''inhibitory'' stimulation. Section VI proposes a brief discussion of the results.

II. MODEL

From the functional or behavioral point of view the synaptic transmission of excitation from cell to cell may be described as follows [2,5]. An input pulse forms a perturbation at the postsynaptic cell called postsynaptic potential (PSP). The excitatory postsynaptic potential (EPSP) depolarizes the membrane bringing neuron to its excitation threshold. When the threshold is reached, the neuron exhibits excitation pulse or action potential. The inhibitory postsynaptic potential (IPSP) hyperpolarizes the neuron tending to decrease its firing activity. The synaptic transmission is unidirectional hence in modeling one can consider the PSP as an external perturbation of the neuron. Let the state (membrane potential) of the single neuron be described by the variable $x(t)=x(t,x_0)$ evolving from some initial conditions $x_0=x(t=0)$. In the simple approximation we may take into account the PSP perturbation by the instant jump (increase for the EPSP and decrease for the IPSP) of the state variable (membrane potential) at time moment t_0 when the input pulse comes. Then, the state of the neuron for $t>t_0$ is given by

$$x(t)=x(t,x_{t_0}), \quad x_{t_0}=x(t,x_0)+u_p. \tag{1}$$

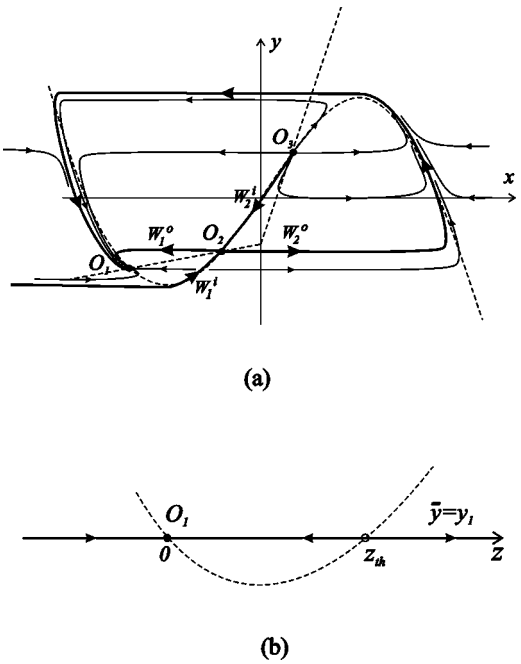

FIG. 1. (a) Qualitative phase portrait of system (2) for $\varepsilon \ll 1$. $W^i_{1,2}$ and $W^o_{1,2}$ denote the incoming and outgoing separatricies of the saddle O_2, respectively. (b) One-dimensional dynamics of Eq. (2) for $\varepsilon \to 0$ at line $\bar{y}=y_1$.

In other words, at $t=t_0$ the input pulse sets the initial conditions for the system. In such an approximation we have ignored the dynamics of the synaptic transmission taking it into account with just one parameter u_p characterizing the ''*strength*'' of synapse. It is positive for EPSP, $u_p>0$, and negative for IPSP, $u_p<0$.

The single neuron dynamics $x(t)$ can be described by the following two-dimensional FitzHugh-Nagumo-like system

$$\begin{aligned} \dot{x} &= f(x)-y, \\ \dot{y} &= \varepsilon[g(x)-y-J], \end{aligned} \tag{2}$$

where $f(x)=x-x^3/3$, $J>0$, and $\varepsilon>0$ and the function $g(x)$ has the form

$$g(x)=\begin{cases} \alpha x, & \text{if } x<0, \\ \beta x, & \text{if } x\geqslant 0. \end{cases}$$

Let the system (2) be in the *excitable* mode. Its phase portrait for $\varepsilon \ll 1$ is shown in Fig. 1(a). The system has three fixed points, $O_1(x_1,y_1)$, $O_2(x_2,y_2)$ and $O_3(x_3,y_3)$. The point O_3 is unstable (node or focus), O_2 is of saddle type, and O_1 is a stable node or focus depending on the parameter values. The stable fixed point O_1 defines the system rest state (rest potential). The incoming separatrix of the saddle, W^i_1, accounts for the excitation threshold (threshold manifold). It means that for a strong enough perturbation exceeding the threshold the system exhibits a long excursion in the phase plane forming the response pulse. Note, that for suitable parameter values the system (2) becomes auto-oscillating with a limit cycle describing periodic sequences of excitation pulses (action potentials) [5].

Let the system (2) get a ''synaptic'' input (1) in the form of a periodic sequence of pulses with the interspike interval τ_p. Each pulse at the time moments $t_n=\tau_p n$, $n=0,1,2,\ldots$, perturbs the current state of the system according to Eq. (1), after that, it evolves autonomously. For example, let the system initially be at rest, i.e., at the fixed point O_1. If the strength of synapse u_p is large enough, then even a single pulse brings the system over the threshold (separatrix W^i_1) and the excitation pulse is generated [Fig. 1(a)]. It is the case of ''strong synapse'' and the system represents a pulse follower. For example, in CNS cerebellar Purkinje cells getting excitatory input from climbing fibers provide a response for sure on each incoming pulse [3]. Let us focus on the opposite situation when u_p is low enough and the system has to accumulate perturbations for some time evoking the response on the definite number of pulses (two, three, etc.). In this case the subthreshold dynamics of (2) plays a major role.

III. NONLINEAR INTEGRATING RESPONSE

Let us consider the system (2) when $\varepsilon \to 0$. Then,

$$\begin{aligned} \dot{x} &= f(x)-y, \\ y &\approx \bar{y}=\text{const}. \end{aligned} \tag{3}$$

If the system (2) initially is at rest (fixed point O_1), then under stimulation (1) its dynamics occurs at the line $\bar{y}=y_1$ and is described by Eqs. (3) [Fig. 1(b)]. Let us assume $x=-1+\xi$. Then, in the interval between the rest point and the threshold point the function $f(x)$ can be represented with its power expansion

$$f(-1+\xi)=-\tfrac{2}{3}+\xi^2+O(\xi^3). \tag{4}$$

In this case, the coordinates of the fixed point O_1 can be obtained explicitly,

$$\begin{aligned} x_1 &= \frac{\alpha-2-\sqrt{\alpha^2-4(\alpha+J-2/3)}}{2}, \\ y_1 &= \frac{\alpha(\alpha-2)-\alpha\sqrt{\alpha^2-4(\alpha+J-2/3)}}{2}-J. \end{aligned} \tag{5}$$

Introducing a new variable $z=x-x_1$ and using Eqs. (3)–(5) one can show that at the line $\bar{y}=y_1$ the dynamics is given by the equation

$$\dot{z}=z^2-zz_{th}, \tag{6}$$

where z_{th} denotes the threshold point [Fig. 1(b)],

$$z_{th}=\sqrt{\alpha^2-4(\alpha+J-2/3)}-\alpha.$$

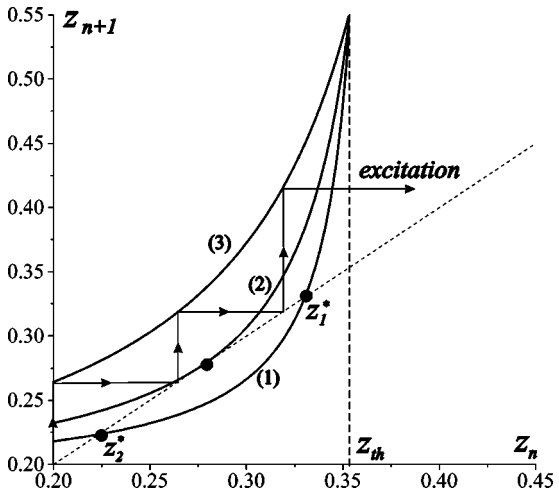

FIG. 2. Behavior of the nonlinear 1D map (8). Parameter values: $\alpha=0.2, J=0.4$. (1) The map has two fixed points, $u_p=0.2, \tau_p=9$. (2) Saddle-node $(+1)$ bifurcation, $u_p=0.2, \tau_p=7.24$. (3) No fixed points, $u_p=0.2, \tau_p=5$. Arrows show the map trajectory corresponding to excitation. Units are arbitrary (a.u.).

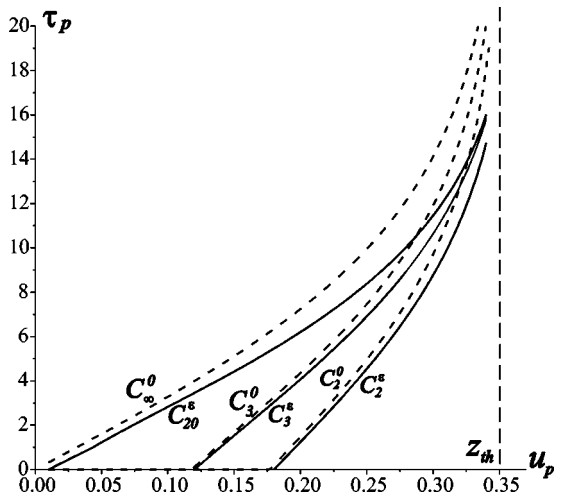

FIG. 3. Parameter plane (u_p, τ_p) illustrating integrating response on pulse stimulation (doublets, triplets, etc.). Dashed curves, C_2^0, C_3^0, C_∞^0, are obtained analytically using the 1D map (8), solid curves, C_2^0, C_3^0, C_∞^0, are calculated numerically using Eq. (2) with $\varepsilon=0.003$. The regions restricted between curves, C_N - C_{N+1} correspond to the response on $N+1$ number of pulses. Parameter values: $\alpha=0.2, J=0.4$. Units are arbitrary (a.u.).

Let the system be stimulated with the interspike interval τ_p. It follows from Eq. (1) that for two neighboring pulses Eq. (6) satisfies the conditions

$$z(t=0)=z_n>0, \quad z(t=\tau_p)=z_{n+1}-u_p>0,$$

where z_n denotes the state of the system when n pulses have been accepted. Then,

$$\tau_p=\int_{z_n}^{z_{n+1}-u_p}\frac{dz}{z^2-zz_{th}} =-\frac{1}{z_{th}}\ln\frac{(z_{n+1}-u_p)(z_n-z_{th})}{z_n(z_{n+1}-u_p-z_{th})}. \tag{7}$$

Here $u_p<z_{th}$, $z_n<z_{th}$, i.e., at the n step the system has not yet reached the threshold. In the interval $[u_p, z_{th}]$ the equation (7) defines 1D nonlinear point map,

$$z_{n+1}=F(z_n)=\frac{z_n[u_p-(u_p+z_{th})\exp(-z_{th}\tau_p)]-u_pz_{th}}{z_n[1-\exp(-z_{th}\tau_p)]-z_{th}}. \tag{8}$$

The behavior of the map (8) is illustrated in Fig. 2. It has two fixed points

$$z_{1,2}^*=\frac{z_{th}+u_p}{2}\pm\sqrt{\frac{(z_{th}+u_p)^2[1-\exp(-z_{th}\tau_p)]-4u_pz_{th}}{4[1-\exp(-z_{th}\tau_p)]}},$$

if the parameters u_p and τ_p satisfy the inequality

$$\tau_p\geqslant\frac{2}{z_{th}}\ln\frac{z_{th}+u_p}{z_{th}-u_p}. \tag{9}$$

The function $F(z_n)$ is monotonically increasing with

$$F'(z_n)=\frac{z_{th}^2\exp(-z_{th}\tau_p)}{\{z_n[1-\exp(-z_{th}\tau_p)]-z_{th}\}^2}>0,$$

It follows from Eq. (8) that $F(u_p)>u_p$, hence $F'(z_2^*)<1$, and the fixed point z_2^* is stable, $F'(z_1^*)>1$ and z_1^* is unstable. Exact equality condition in Eq. (9) indicates saddle node or $+1$ bifurcation resulting in the disappearance of the fixed points (Fig. 2). The inequality (9) defines the region in the parameter plane (u_p, τ_p) shown in Fig. 3. It is located above the boundary curve C_∞^0. Here the system does not respond to the stimulation at all because all trajectories of the map are attracted by the stable fixed point z_2^* located below the threshold. Note that in this region, the characteristic relaxation time of the system is much shorter than the interspike interval, hence it has enough time to recover its rest state until the next pulse in the sequence has come.

When the map (8) has no fixed points, its trajectories after some number of steps N, overcome the threshold, $z_N>z_{th}$. It means that the system responds on N-pulse message. Let us consider a doublet stimulus $N=2$. Using the map (8) with initial conditions $z_1=u_p$ one can show that the condition $z_2>z_{th}$ is satisfied if the parameter values satisfy the inequality

$$0<\tau_p<\tau_p^2=\frac{2}{z_{th}}\ln\frac{u_p}{z_{th}-u_p}. \tag{10}$$

In Fig. 3 this region is located below the curve C_2^0. Similarly, the system responds on a triplet, $z_3>z_{th}$, if

$$\tau_p^2<\tau_p<\tau_p^3=\frac{1}{z_{th}}\ln\frac{u_p(z_{th}+u_p)}{(z_{th}-u_p)^2}. \tag{11}$$

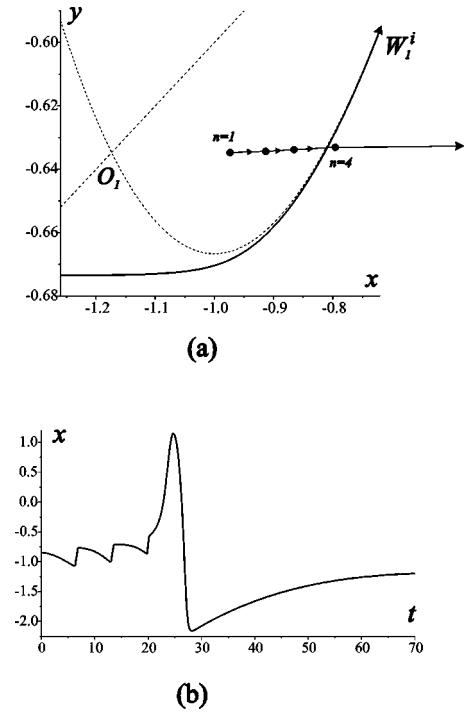

FIG. 4. A response on $N=4$ pulse message. (a) The map trajectory in the phase plane. (b) Time evolution of the system (2). Parameter values: $\alpha=0.2$, $\beta=10$, $J=0.4$, $\varepsilon=0.1$, $u_p=0.33$, and $\tau_p=6.8$. Units are arbitrary (a.u.).

This inequality defines the region located between the curves C_2^0 and C_3^0 (Fig. 3). By increasing the number of pulses one can obtain the sequence of boundary curves C_N^0 accumulating to C_∞^0 with $N\to\infty$.

To verify the results Fig. 3 also shows the curves C_N^ε obtained in numerical simulation of the system (2) with Eq. (1) for $\varepsilon=0.003$. Here the curve C_{20}^ε estimates the boundary curve C_∞^ε. There is a good agreement between the analytical and numerical results. Growing difference between the curves with increasing N and u_p can be explained using the phase portrait of system (2) (Fig. 1). For nonzero ε the variable $y(t)$ is slightly increasing below the nullcline $g(x)-J$ bringing the system to the region below the fixed point O_1, $x<x_1$ (refractory state). Then, to overcome the threshold the value of u_p should be higher at the next coming pulse. Thus, in the parameter plane (u_p,τ_p) the curves C_N^ε goes below than the corresponding curves C_N^0.

Let us fix the parameter u_p characterizing the ''strength'' of the EPSP (1). Then, for variable characteristic of the external signal (interspike interval τ_p) the system can select the doublets, triplets, and more complex messages summarizing or *integrating* them in the single response pulse. For illustration, the four-pulse response is shown in Fig. 4. As expected, the trajectory of the map (8) lies near the line $\overline{y}=y_1$ and jumps over the threshold at $N=4$ [Fig. 4(a)]. Figure 4(b) shows time evolution of the system (2). To be excited it accumulates (integrates) perturbations below the threshold. To describe further evolution of the system (not considered here) one must take into account the response pulse duration and the refractory period.

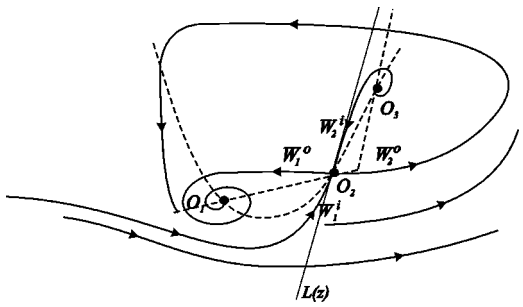

FIG. 5. Qualitative phase portrait of the system (2) when it has oscillatory dynamics near the fixed point O_1. The tangent line $L(z)$ approximates the separatrix (threshold manifold) W_1^i near the fixed point O_2.

In possible applications of the model such selectivity to a number of input pulses can be used when designing the unit of a *conventional neurocomputer*. It represents a network of many intercoupled cells with programmable connections and makes processing by means of temporal summation or integration of incoming signals [16].

IV. RESONANT RESPONSE

For suitable parameter values (for example, for increasing ε) the fixed point O_1 of system (2) acquires oscillatory properties (Fig. 5). Let us suppose that it is a stable focus with eigenvalues $\lambda_{1,2}=-h\pm I\omega$,

$$h=\frac{\varepsilon-f_{x1}}{2}>0,\quad \omega=\sqrt{\varepsilon(\alpha-f_{x1})-\frac{(f_{x1}-\varepsilon)^2}{4}}, \tag{12}$$

with $f_{x1,\,x2}=1-x_{1,2}^2$, respectively. Hence, near the rest point the system (2) displays damped oscillatory behavior.

A. Linear approximation

First, let us consider a linear approximation of the system (2) when it evolves below the threshold. Linearizing Eq. (2) near the fixed point O_1 we obtain

$$\begin{aligned}\dot{z}&=f_{x1}z-w,\\ \dot{w}&=\varepsilon(\alpha z-w),\end{aligned} \tag{13}$$

with $z=x-x_1$ and $w=y-y_1$. Initial conditions for Eqs. (13) are defined by Eq. (1). Then, for two neighboring pulses

$$\begin{aligned}&z(t=0)=z_n,\quad w(t=0)=w_n,\\ &z(t=\tau_p)=z_{n+1}-u_p, w(t=\tau_p)=w_{n+1},\end{aligned} \tag{14}$$

where the point (z_n,w_n) defines the state of the system when n pulses have been accepted. Solving linear problem Eqs. (13)–(14) yield the following two-dimensional linear point map

$$\begin{aligned}z_{n+1}&=az_n+bw_n+u_p,\\ w_{n+1}&=cz_n+dw_n,\quad n=1,2,\ldots,\end{aligned} \tag{15}$$

with

$$a=\exp(-h\tau_p)\left[\cos(\omega\tau_p)+\frac{f_{x1}+h}{\omega}\sin(\omega\tau_p)\right],$$

$$b=-\exp(-h\tau_p)\frac{\sin(\omega\tau_p)}{\omega},$$

$$c=\exp(-h\tau_p)\left(\omega+\frac{(f_{x1}+h)^2}{\omega}\right)\sin(\omega\tau_p),$$

$$d=\exp(-h\tau_p)\left[\cos(\omega\tau_p)-\frac{f_{x1}+h}{\omega}\sin(\omega\tau_p)\right].$$

The single fixed point of the map. (15) has the coordinates

$$z^*=\frac{u_p(1-d)}{(1-a)(1-d)-bc},\quad w^*=\frac{u_pc}{(1-a)(1-d)-bc},$$

and the multipliers

$$\mu_{1,2}=\exp[(-h\pm I\omega)\tau_p]). \tag{16}$$

Hence the fixed point is a stable focus that attracts all the trajectories of the linear point map (15).

For simplicity, let us approximate the threshold manifold W_1^i by the following linear function,

$$w=L(z)=-y_1+(f_{x2}-\lambda_{x2})(z+x_1), \tag{17}$$

$$\lambda_{x2}=\frac{f_{x2}-\varepsilon}{2}-\sqrt{\frac{(f_{x2})-\varepsilon)^2}{4}-\varepsilon(\alpha-f_{x2})}.$$

It is tangent to the separatrix at the fixed point O_2 (Fig. 5). Let the system initially be at rest, hence $z_1=u_p, w_1=0$. The excitation threshold for single pulse perturbation, $n=1$, is given by

$$\overline{z_{th}}=-x_1+\frac{y_1}{f_{x2}-\lambda_{x2}}.$$

For $u_p<\overline{z_{th}}$ iterating the map (15) with the initial conditions one can obtain the point (z_N,w_N). Then, the inequality

$$w_N<L(z_N),$$

ensures that the system evokes response on N pulses in the sequence. Figure 6 illustrates the response regions for doublets D_2, and triplets D_3, in the parameter plane (u_p,τ_p). The dashed curve C_∞, binds the region below the curve corresponding to the fixed point located above the threshold, $w^*<L(z^*)$. Since it is a stable focus and all the trajectories are attracted, this inequality provides sufficient conditions for excitation. Note that when it lies below the threshold $w^*>L(z^*)$, the trajectories can reach the threshold and the system can be excited at some number of pulses (Fig. 6).

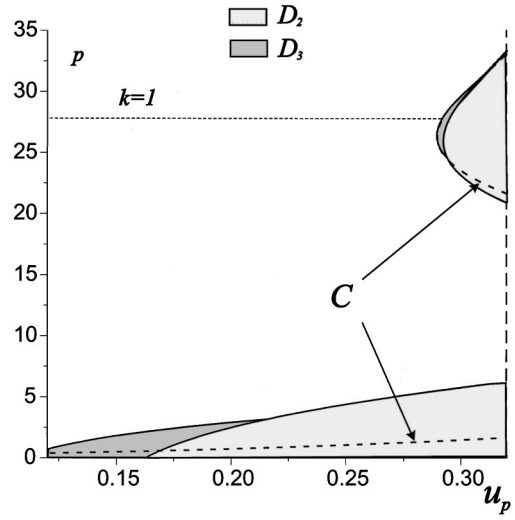

FIG. 6. Resonant response in linear approximation. The regions of doublet and triplet response are filled with light and dark gray colors, respectively. The curve C_∞ corresponds to the location of the fixed point (z^*,w^*) of the map (15) at the threshold line $L(z)$. Parameter values: $\alpha=0.5$, $J=0.15$, and $\varepsilon=0.1$. Units are arbitrary (a.u.).

Since the system (2) has oscillatory properties the response regions (Fig. 6) appear in a resonance way. The linear resonance relation for damped oscillation near the point O_1 is

$$\tau_p^k=\frac{2\pi k}{\omega}, k=1,2,\ldots, \tag{18}$$

If it is satisfied, the map (15) splits into a pair of linear one-dimensional maps

$$z_{n+1}=\exp(-h\tau_p^k)z_n+u_p,$$

$$w_{n+1}=\exp(-h\tau_p^k)w_n,$$

with the stable fixed point

$$z^{*k}=\frac{u_p}{1-\exp(-h\tau_p^k)},\quad w^{*k}=0. \tag{19}$$

In this case the sufficient conditions for excitation becomes $z^{*k}>\overline{z_{th}}$. Using Eqs. (17) and (19) we find that for response at exact resonance

$$u_p>u_p^k=\overline{z_{th}}[1-\exp(-h\tau_p^k)]. \tag{20}$$

It shows that, for damped oscillation the resonance regions exponentially decay for increasing k (Fig. 6). Note that the regions (their maxima) are slightly shifted relative to τ_p^k in the result of the finite slope of the line $L(z)$ approximating the threshold (Fig. 5).

B. Nonlinear resonance response

Let us now take into account nonlinearity of the system (2). Along with the appearance of the resonance behavior

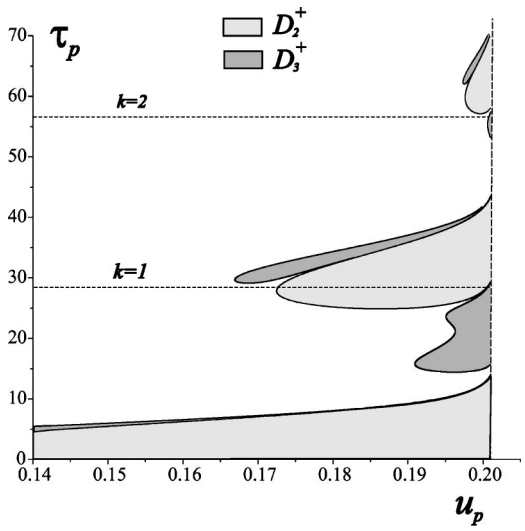

FIG. 7. Nonlinear resonant response regions, D_2^+ and D_3^+, corresponding to the doublet and triplet EPSP stimuli, respectively. Parameter values: $\alpha=0.5$, $J=0.15$, and $\varepsilon=0.1$. Units are arbitrary (a.u.).

predicted by linear theory one may expect various nonlinear effects including a shift of the response curves and responses at composite frequencies. In particular, for higher values of u_p when approaching the separatrix W_1^i the oscillation becomes nonisochronous and the system evolves for a long time near the separatrix threshold. Furthermore, the separatrix itself is given by a nonlinear curve (Fig. 5).

The trajectories of the system (2) with the conditions (14) define nonlinear map F, $(z_n,w_n)\rightarrow(z_{n+1},w_{n+1})$. For the particular trajectory the function F can be derived by numerical integration of Eqs. (2). If after N steps the trajectory jumps over the separatrix W_i^1 (also numerically calculated), then the system responds to N-pulse message. Figure 7 illustrates the response regions for doublets D_2^+ and triplets D_3^+. As expected the structure of the bifurcation set has resonance character with exponential decay (20), but it is quite different from that obtained in linear approximation. The curves for triplet response at $k=2,3$ form two separate regions. Furthermore, the system may respond to either doublets or triplets for values of τ_p that are even antiphase (18) according to the linear theory. This is the result of nonisochronous behavior.

Note that the response on increasing number of pulses ($N=4,5,\ldots,$) becomes more complicated. It is also restricted within a number of separate regions (not shown here). For example, the behavior of the 2D nonlinear map obtained numerically at some point in the (u_p,τ_p) plane for $N=8$ is illustrated in Fig. 8(a). Before reaching the threshold the trajectory behaves quite complex. Time evolution of the system (2) is shown in Fig. 8(b). Here the excitation pulse (action potential) appears after long lasting subthreshold oscillation.

Thus, excitable systems with oscillatory subthreshold behavior even when the oscillations are damped can provide a selective communication with nonlinear *resonant* properties. There are separate regions of selective response on messages with definite number of pulses, hence the system is nonlinear

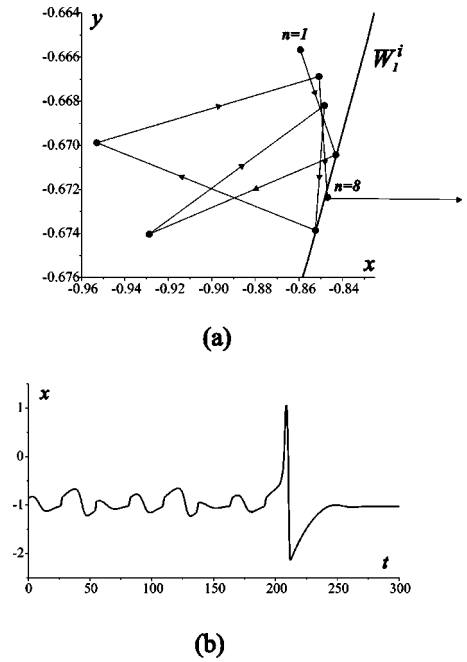

FIG. 8. Resonant response of the system (1) and (2) integrating the message of $N=8$ EPSP pulses. Parameter values: $\alpha=0.5$, $\beta=10$, $J=0.15$, $\varepsilon=0.1$, $u_p=0.172$, and $\tau_p=27.5$. (a) The trajectory of the nonlinear map F leading to excitation. (b) Time evolution of the system (2). Units are arbitrary (a.u.).

integrator as well. In possible applications the model may be useful in the design of an *oscillatory neurocomputer*. Its processing functions are based on resonance communication between the units (neurons) and their connectivity [16].

V. NONLINEAR RESPONSE ON IPSP

Many neurophysiological experiments have shown that neurons when stimulated may fire at hyperpolarized state [3,4]. It means that inhibition of the cell (IPSP) may also cause an action potential. Qualitative models have explained such possibility by complex behavior of the threshold manifold or by the presence of the second excitation threshold at the hyperpolarized state [4,5]. The models (1) and (2) may also exhibit nonlinear integrating and resonant response on the IPSP. Note that in the region $x<x_1$ of the phase plane the separatrix W_i^1 (threshold manifold) goes up (Fig. 5) providing the possibility of excitation caused by ''inhibition,'' $u_p<0$. The regions of the IPSP response on doublets (D_2^-) and triplets (D_3^-) numerically calculated are presented in Fig. 9. Their structure is quite similar to that obtained for the EPSP stimulation. The triplet response occurs near the doublet within two separate regions at each resonance number, $k=2,3$. Then, for variable interspike interval τ_p, the system responds on definite number of pulses coming at selective frequencies. Note that more complex response may occur in the neighborhood of $D_{2,3}^-$. For illustration, the trajectory of the nonlinear map and time evolution of the system when responding on $N=12$ number of the IPSP stimuli are shown in Figs. 10(a) and 10(b), respectively.

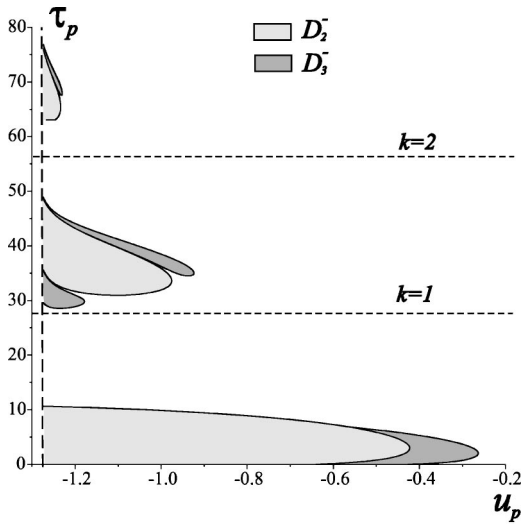

FIG. 9. Nonlinear resonant response on the IPSP stimuli. The regions D_2^+ and D_3^+ correspond to the response on doublet and triplet messages, respectively. Parameter values: $\alpha=0.5$, $J=0.15$, and $\varepsilon=0.1$. Units are arbitrary (a.u.).

VI. DISCUSSION

The paper has discussed some problems of communication and information processing by excitable systems. The FitzHugh-Nagumo-like model with a threshold manifold based on *functional* properties of neurons is investigated. It has been shown that the analysis of the system response to information messages taken here as simple periodic sequences of pulses and packages of two, three or more pulses with a characteristic interspike interval may be reduced to the analysis of transient trajectories and limit sets of 1D and 2D linear and nonlinear point maps. The bifurcation sets illustrating different responses have been obtained and analyzed. It is shown that if the system has relaxation subthreshold dynamics the response appears when integrating the definite number of spikes. The regions of the response have been analytically estimated and numerically verified. When the dynamics is oscillatory, the system responds integrating signals at the selective frequencies. The response is characterized by both oscillations near rest point and by the nonlinear behavior near the threshold manifold. Moreover, the system may selectively respond on the inhibitory stimuli. Either type of the response is defined by the dynamics of the system (nonisochronous damped oscillation) and by the characteristics (strength and sign) of the ''synaptic'' input.

In summary, the excitable system modeling single neuron dynamics even taken apart from neuron assemblies may exhibit various information processing features including integration, selection on frequency, and integration at selective frequencies. Hence, it is, in fact, a *minimal processing unit*. The next task will be the integration of such units in networks to reproduce various functions of CNS such as processing of visual information, associative memory, etc. In difference with various neural network models (oscillatory networks, conventional networks, cellular neural networks, reaction diffusion lattices, etc.) the assemblies of excitable units might exhibit processing at single ''cell level.'' Such units, of course, have relatively complex internal dynamics, but display clear functions.

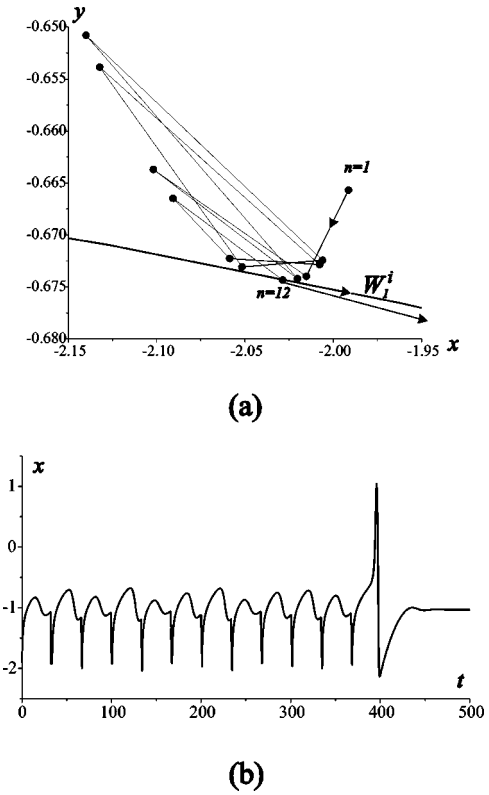

FIG. 10. Resonant integration of a complex ($N=12$) message of the IPSP pulses. Parameter values: $\alpha=0.5$, $\beta=10$, $J=0.15$, $\varepsilon=0.1$, $u_p=-0.96$, and $\tau_p=33.5$. (a) The trajectory of the nonlinear map F leading to excitation. (b) Time evolution of the system (2). Units are arbitrary (a.u.).

ACKNOWLEDGMENTS

I am grateful to Professor V.I. Nekorkin, Professor M.G. Velarde, Professor R. Llinas, and Dr. V.I. Makarenko for valuable discussions. This research has been supported by the Russian Foundation for Basic Research under Grants Nos. 01-02-06359 and 00-02-16400 (Russia).

[1] J.D. Murray, *Mathematical Biology*, 2nd Corrected ed. (Springer-Verlag, Berlin, 1993).

[2] *Principles of Neural Science*, 3rd ed., edited by E.R. Kandel, J.H. Schwartz, and T.M. Jessell (Appleton and Lange, Norwalk, Connecticut, 1991).

[3] R. Llinas, Science **242**, 1654 (1988); R. Llinas, *Oscillations in CNS Neurons: A Possible Role for Cortical Interneurons in the Generation of 40-Hz Oscillations*, Induced Rhythms in the Brain, edited by E. Basar and T. Bullock (Birkhauser, Berlin, 1991); R. Llinas and Y. Yarom Y, J. Physiol. (London) **376**,

163 (1986).
[4] N. Schweighofer, K. Doya, and M. Kawato, J. Neurophysiol. **82**, 804 (1999).
[5] E.M. Izhikevich, Int. J. Bifurcation Chaos Appl. Sci. Eng. **10(6)**, 1171 (2000).
[6] M.C. Eguia, M.I. Rabinovich, and H.D.I. Abarbanel, Phys. Rev. E **62**, 7111 (2000).
[7] N. Brenner, S.P. Strong, R. Koberle, W. Bialek, and R.R. de Ruyter van Steveninck, Neural Comput. **12**, 1531 (2000).
[8] R. Stoop, K. Schindler, and L.A. Bunimovich, Nonlinearity **13**, 1515 (2000).
[9] A. Babloyantz and C. Lourenco, Proc. Natl. Acad. Sci. U.S.A. **91**, 9027 (1994).
[10] J.J. Hopfield, Proc. Natl. Acad. Sci. U.S.A. **79**, 2554 (1982).
[11] V.I. Nekorkin, V.B. Kazantsev, M.I. Rabinovich, and M.G. Velarde, Phys. Rev. E **57**, 3344 (1998).
[12] L.F. Abott, J. Phys. A **23**, 3835 (1990).
[13] E. Bagarinao and C. Saloma, Phys. Rev. E **54**, 5516 (1996).
[14] A.H.L. West and D. Saad, Phys. Rev. E **57**, 3265 (1998); J.W. Kim and H. Sompolinsky, *ibid.* **58**, 2348 (1998).
[15] R. Rodriguez and H.C. Tuckwell, Phys. Rev. E **54**, 5585 (1996).
[16] F.C. Hoppensteadt and E.M. Izhikevich, Phys. Rev. Lett. **82**, 2983 (1999); F.C. Hoppensteadt and E.M. Izhikevich, Phys. Rev. E **62**, 4010 (2000).
[17] S. Grillner, Sci. Am. (Int. Ed.) **64**, (1991).
[18] G. Manganaro, P. Arena, and L. Fortuna, *Cellular Neural Newtworks. Chaos, Complexity and VLSI Processing* (Springer-Verlag, Berlin, 1999).
[19] V.I. Nekorkin, V.B. Kazantsev, and M.G. Velarde, Eur. Phys. J. B **16**, 147 (2000).
[20] V.A. Makarov, V.I. Nekorkin, and M.G. Velarde, Phys. Rev. Lett. **86**, 3431 (2001).